PROCEEDINGS B

royalsocietypublishing.org/journal/rspb

Research

Cite this article: Seebens H, Briski E, Ghabooli S, Shiganova T, MacIsaac HJ, Blasius B. 2019 Non-native species spread in a complex network: the interaction of global transport and local population dynamics determines invasion success. *Proc. R. Soc. B* **286**: 20190036.
http://dx.doi.org/10.1098/rspb.2019.0036

Received: 6 January 2019
Accepted: 5 April 2019

Subject Category:
Ecology

Subject Areas:
ecology, computational biology

Keywords:
propagule pressure, metapopulation, invasive species, modelling, ballast water release, global shipping

Author for correspondence:
Hanno Seebens
e-mail: hanno.seebens@senckenberg.de

Electronic supplementary material is available online at https://dx.doi.org/10.6084/m9.figshare.c.4467431.

THE ROYAL SOCIETY PUBLISHING

Non-native species spread in a complex network: the interaction of global transport and local population dynamics determines invasion success

Hanno Seebens[1,2], Elizabeta Briski[3], Sara Ghabooli[4], Tamara Shiganova[5], Hugh J. MacIsaac[4] and Bernd Blasius[2,6]

[1]Senckenberg Biodiversity and Climate Research Centre (BiK-F), Senckenberganlage 25, 60325 Frankfurt am Main, Germany
[2]Institute for Chemistry and Biology of the Marine Environment, Carl-von-Ossietzky University, Carl-von-Ossietzky Straße 9-11, 26111 Oldenburg, Germany
[3]GEOMAR Helmholtz-Zentrum für Ozeanforschung Kiel, Düsternbrooker Weg 20, 24105 Kiel, Germany
[4]Great Lakes Institute for Environmental Research, University of Windsor, Windsor, Ontario, Canada N9B 3P4
[5]Shirshov Institute of Oceanology, Russian Academy of Sciences, 36, Nakhimovskiy Prospect, Moscow 117997, Russia
[6]Helmholtz Institute for Marine Biodiversity at the University Oldenburg (HIFMB), Ammerländer Heerstraße 231, 26129 Oldenburg, Germany

HS, 0000-0001-8993-6419; EB, 0000-0003-1896-3860

The number of released individuals, which is a component of propagule pressure, is considered to be a major driver for the establishment success of non-native species. However, propagule pressure is often assumed to result from single or few release events, which does not necessarily apply to the frequent releases of invertebrates or other taxa through global transport. For instance, the high intensity of global shipping may result in frequent releases of large numbers of individuals, and the complexity of shipping dynamics impedes predictions of invasion dynamics. Here, we present a mathematical model for the spread of planktonic organisms by global shipping, using the history of movements by 33 566 ships among 1477 ports to simulate population dynamics for the comb jelly *Mnemiopsis leidyi* as a case study. The degree of propagule pressure at one site resulted from the coincident arrival of individuals from other sites with native or non-native populations. Key to sequential spread in European waters was a readily available source of propagules and a suitable recipient environment. These propagules were derived from previously introduced 'bridgehead' populations supplemented with those from native sources. Invasion success is therefore determined by the complex interaction of global shipping and local population dynamics. The general findings probably hold true for the spread of species in other complex systems, such as insects or plant seeds exchanged via commercial trade or transport.

1. Introduction

The introduction of non-native species into new locales is one of the greatest threats to biodiversity [1], and the global spread of species has strongly increased during the last decades [2]. This is mainly a consequence of the globalization of trade and transport as many species are accidentally carried by means of global transportation [2]. The complexity of current transport dynamics can lead to complex movement patterns of non-native species, even for a single transportation mode. For example, the release of ballast water by cargo ships is one of the world's largest transport vectors of species [3] and the large number of individual ship movements leads to complicated dynamics of how species in ballast tanks are dispersed. The high variability in transport dynamics can have pronounced effects on the number of released individuals at

a certain site and thus on establishment success [4]. However, the interaction of these large-scale spreading dynamics on local establishment success is less understood.

The invasion success of a species, expressed as the establishment of a new population at a non-native locale, depends on various factors, but a reliable predictor across taxonomic groups and studies is the number of released individuals, which is the propagule pressure [5,6]. Low propagule pressure often leads to a disproportionally low probability of establishment owing to e.g. Allee effects or environmental stochasticity [7], whereas increasing propagule pressure is associated with increased invasion success [8]. The relationship between these variables can be formulated as a dose–response or risk–release relationship [9]. The drivers of the propagule pressure and the shape of the risk–release relationship are of considerable practical interest as it may inform the effort required to reduce invasion risk [9]. The concepts of propagule pressure and Allee effects suggests that a threshold of propagule pressure is required to overcome negative population growth at low population density, but this threshold can vary considerably in space and time owing to e.g. environmental mismatches and biotic interactions [10]. In addition, propagule pressure is a function of strength and frequency of invasion events and thus can strongly fluctuate over time [6].

The process of biological invasions has often been simplified to the release of individuals at a specific time at one site, which allows analysis of invasion success based on this single founding population [8]. While this may be a realistic assumption for cases involving large organisms like the intentional introduction of vertebrates (e.g. fishes, birds), it is insufficient for species that are released on a quasi-continuous rate at multiple sites [4]. For instance, a high shipping intensity between two ports can result in a high rate of exchange of species living at these ports. A single release event may not be sufficient for the establishment, but the regular release of individuals of the same species may result in the growth of the founding population to a size that is high enough to overcome the disadvantages of small founding populations. This may also be the case if ships travel along different routes, originate from different ports or have varying numbers of intermediate stops. Consequently, the success of an invasion—defined here as the establishment of a non-native population—in such a complex network is determined by the combined effect of the total number of released individuals at a port during a given time period and the population dynamics at the recipient site. Although studies have analysed the global spread of species by ships using information on the last port of call [11,12], the network of shipping trajectories has rarely been taken into account to simulate global spread dynamics (but see [13]). Furthermore, the spatio-temporal dynamics of propagule pressure and the consequences for a successful invasion in complex networks remain poorly understood.

Here, we present a modelling study to analyse the interaction of global transportation and local population dynamics. In particular, we are interested in (i) how the movement of individuals in a complex network influences the variation in propagule pressure in space and time, and (ii) how this spatio-temporal variation in propagule pressure affects establishment success.

As a case study, we use the introduction of the comb jelly *Mnemiopsis leidyi* from North America into European waters by ballast water of ships. *Mnemiopsis leidyi* is native to the Atlantic coastal waters of North and South America and was first reported in the Black Sea in the early 1980s [14]. In 1990, the species was recorded in the Aegean Sea [15]. The species was then reported in other parts of the eastern (1992) and then western Mediterranean Sea (2005), and subsequently in the Baltic (2006) and North Seas (2006) [16–19]. Recently, the genetic diversity of native and non-native populations was analysed by four studies [20–23]. The first two suggested that *M. leidyi* was introduced independently to northern (North, Baltic Seas) and southern Europe (i.e. Black, Azov and Caspian Seas). The latter two studies analysed the pathways of introduction to the Mediterranean Sea. Bolte *et al.* [23] assumed introductions only from the Black Sea, while Ghabooli *et al.* [21] concluded the possibility of introduction from both the native region and the Black Sea. *Mnemiopsis leidyi* almost certainly was introduced by ship's ballast water [22,24].

We first present a novel mathematical model for the spread of marine planktonic species among ports transported by ballast water of cargo ships, thereby explicitly accounting for the interaction of Allee effects and environmental conditions. Using nearly three million ship movements, the model simulates the population dynamics of *M. leidyi* in *ca* 1500 ports worldwide, and in ballast water tanks of greater than 33 000 ships. In a second step, the set of best-fitting models was used to analyse spreading dynamics and to determine spatio-temporal variation in propagule pressure leading to a successful invasion. Finally, we establish risk–release curves for different scenarios to analyse variation among sites and the reliability of the observed curves. We show that the complexity in transportation can lead to counterintuitive spatio-temporal developments of propagule pressure and establishment success.

2. Material and methods

(a) Environmental data

We approximated food availability for *M. leidyi* by nutrient concentrations such as phosphorus, nitrate and silicate, which represent important drivers of primary productivity [25]. We obtained global data for mean annual temperature, salinity, nitrate, phosphate and silicate from the World Ocean Atlas (WOA, www.nodc.noaa.gov). We extracted the minimum annual sea surface temperature from monthly temperature data provided by WOA. For most ports, salinity was recalculated from water density data provided by IHS Fairplay (www.ihsfairplay.com; now www.ihs.com) and water temperature. If these data were not available, we obtained salinity from WOA. A more detailed description of the salinity calculation can be found in Seebens *et al.* [26].

(b) Shipping data

Data of global ship movements were obtained as arrival and departure dates of 33 566 cargo ships larger than 10 gross tonnes, operating during 2007–2008 between 1477 ports worldwide. This information was used to reconstruct travel routes for each individual ship during that time period on a daily basis [27]. Altogether, the final dataset contained 2 934 610 individual ship movements between two ports. The date of arrival and departure was recorded by the Automatic Information System and was provided by IHS Fairplay. To simulate longer time periods, ship movements were repeated after 2 years. Because the database contained less information on ship

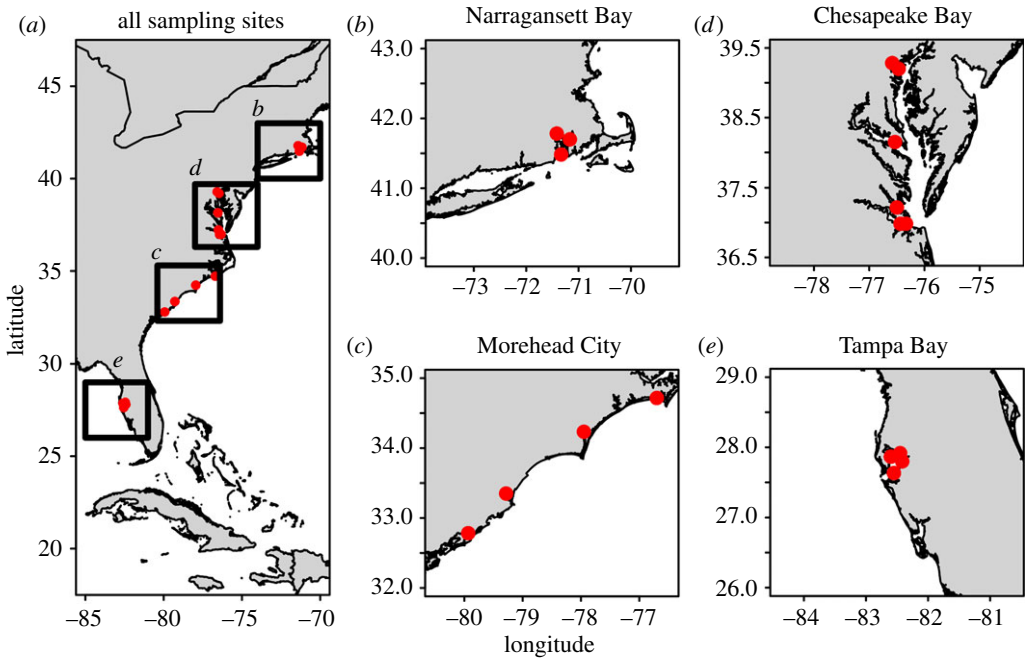

Figure 1. The distribution of ports located in the native region along the east coast of the USA (*a*) and within each of the four regions considered as the starting points of spread of *M. leidyi* (*b*–*e*).

movement at the edge of this time window, this caused a recurrent drop in propagule pressure every 2 years (see Results), which, however, should not affect overall results.

In addition, ship-specific information such as the cargo-carrying capacity was also reported. The ship's carrying capacity measured in deadweight tonnes was used to estimate the total ballast tank volume of a ship. According to published lists of ship sizes and ballast tank capacities for different ship types [28], total ballast tank volume was on average one-fifth of the ship's carrying capacity. We adopted this relationship and calculated total ballast tank volume in m^3 (i.e. tonnes) for each ship type and ship size accordingly (electronic supplementary material, figure S1). The network of all shipping trajectories was described in more detail in Kaluza *et al.* [27] and the calculation of ballast tank capacities was presented in Seebens *et al.* [26].

(c) Genetic data

Ghabooli *et al.* [20,21] investigated sequence variation in the nuclear ribosomal internal transcribed spacer (ITS) region of 16 native and non-native populations of *M. leidyi* in America and Europe. Genetic differentiation among populations was measured using pairwise F_{st}. We removed three sample sites (Caspian Sea and South America) for which shipping data were lacking. We aggregated sites located close to each other to match the resolution of ship movement data. Our final dataset included four native sites distributed evenly along the east coast of the USA (Narragansett Bay, Rhode Island; Tampa Bay, Florida; Chesapeake Bay, Virginia; Morehead City, North Carolina) (figure 1) and five invaded sites in Europe (Black Sea, Baltic Sea, and three sites in the Mediterranean Sea at the coasts of Israel, France and Spain). F_{st} values were averaged between these sites such as to obtain an F_{st} matrix with native sites as rows and invaded sites as columns (electronic supplementary material, table S1). Reusch *et al.* [22] conducted a similar type of analysis using microsatellites, though they sampled populations different from Ghabooli *et al.* resulting in a lower number of sites matching our ship data. We performed the same modelling approach using data from Reusch *et al.* but as the overall results did not deviate distinctly from those using data from Ghabooli *et al.*, we presented results only using the latter.

(d) Model

We modelled the population dynamics of *M. leidyi* using ordinary differential equations (ODE) for each port and ship, which resulted in 35 043 ODEs. As the importance of adaptation of *M. leidyi* to local environmental conditions for the invasion of European sites was unclear, we investigated three different model versions: (i) we ignored environmental conditions (invasion driven only by population dynamics and shipping); (ii) we assumed that *M. leidyi* is adapted to the mean environmental conditions of the full native range (one ecotype); and (iii) we considered four ecotypes, each adapted to the local environmental conditions of the sampled regions. For the sake of simplicity, we assumed that environmental preferences of ecotypes were retained (no local adaptation). We performed an extensive model selection procedure to identify the model that best fitted the observed data. The best-fitting model was then used to investigate relationships between propagule pressure, environmental conditions and establishment success.

The model was intentionally kept simple for aspects specific to ballast water transport or population dynamics of *M. leidyi*. These simplifications were necessary to facilitate a general understanding of the observed dynamics under investigation. We modelled *M. leidyi*'s population dynamic in a port i using a logistic growth function that incorporated an Allee effect, extended by a mortality term $\mu_i N_i$ [29]:

$$\dot{N}_i = rN_i(k - N_i)(N_i - a) - \mu_i N_i, \tag{2.1}$$

with N_i being the population density in individuals m^{-3} in port i, r the growth rate (assumed to be identical in all ports), k the carrying capacity in the case of a perfect environmental match ($\mu_i = 0$) and a the Allee threshold (i.e. the density below which the population experiences negative growth due to an Allee effect) in the case of perfect environmental match. Here, we refer to the Allee effect in its broader sense, capturing all kinds of mechanisms which might lead to an increased probability of

extinction at low density, including demographic and environmental stochasticity [30], which play an important role even for parthenogenetic species such as *M. leidyi*. The within-port mortality μ_i linearly scales with environmental mismatches of species requirements and local conditions or was set constant if no environmental factors were considered. A low environmental match would result in high mortality at that port (see below).

The model had two equilibria: an unstable equilibrium at a and a stable one at k if $\mu_i = 0$ (electronic supplementary material, figure S2). An increase in $\mu_i > 0$ would result in a change of the equilibria, which we then denoted as the realized critical density a_{real} and the realized carrying capacity k_{real}. That is, while a and k were kept constant, a_{real} and k_{real} depend on μ_i and thus indirectly on environmental matches. A mismatch with optimal environmental conditions (i.e. higher μ_i) would give rise to an elevated a_{real} and a lower k_{real}, and thus a lower probability to establish a new population (electronic supplementary material, figure S2). The realized critical density a_{real} can be regarded as a barrier which has to be overcome by the species for successful invasion. Note that a_{real} depended on local environmental conditions and thus was location-specific. We calculated a_{real} by solving equation (2.1) for $\dot{N} = 0$ using the parameters of the best-fitting model (see below).

To incorporate environmental conditions, we let μ_i depend on the environmental mismatch between environmental conditions in the ports and the preferences of the species or ecotype. The mortality μ_i owing to environmental mismatches was calculated as follows:

$$\mu_i = \frac{1}{n}\sum_{e=1}^{n} \mu_e |X_i^e - X_{\text{spec}}^e|, \tag{2.2}$$

with X_i^e denoting the value of a standardized environmental parameter e of the port i, X_{spec}^e the value of the optimal condition of the species or the ecotype and μ_e the relative contribution of parameter e to the overall mortality. As environmental factors e, we used annual mean values of water temperature and salinity, nitrate, phosphate and silicate as proxies for productivity, and minimum winter temperature of the respective regions. We tested the model with all possible combinations of environmental parameters.

Populations S_k of *M. leidyi* in ballast tanks of ship k were assumed to decrease exponentially with mortality rate μ_k [31,32] according to

$$\dot{S}_k = -\mu_k S_k, \tag{2.3}$$

where μ_k was assumed to be constant for all ships.

Each time a ship k entered a port i, it was assumed that ballast water was discharged, which resulted in a release of *M. leidyi* individuals if $S_k > 0$. For simplicity, we assumed that the same amount of ballast water, which was released, was also uploaded, and thus the total amount of water did not change in ports or ballast tanks. Although the populations N and S were modelled as densities of individuals, the exchange of individuals between ports and ships necessitated the calculation of total numbers of individuals, which was done as follows (electronic supplementary material, figure S3): For simplicity, the volume of released or uploaded ballast water was assumed to be a constant proportion s of the total capacity of ballast water tanks v_k of the ship. The capacity of ballast water tanks was a function of the ship's carrying capacity as described above (see 'Shipping data'). Thus, sv_k denoted the volume of discharged or uploaded ballast water and sv_kS_k was the number of released individuals by ship k if it was entering a port on that day. After summing up over all ships k_i entering port i on a given day and dividing by the port volume v_i (considered here to be constant for all ports), the density of individuals I_i released by all ships entering the port on this day was given by

$$I_i = \frac{1}{v_i}\sum_{k_i} sv_{k_i}S_{k_i}. \tag{2.4}$$

This immigration term was simultaneously added once per day to the population density N_i in equation (2.1). That is, numerically the differential equation (2.1) was solved in bursts of one day length. At the end of each simulation burst, population densities N_i were increased to the new values $N_i + I_i$, which were then taken as initial density for the simulation burst of the successive day. We assumed that the removal of individuals from port water owing to ballast water uptake did not influence species densities in ports as this influence should be vanishingly small. We therefore did not include an emigration term in the calculation of N_i.

Likewise, we calculated the immigration of individuals I_k from the port into the ship's ballast tanks and the emigration E_k out of a ship:

$$I_k = \frac{1}{v_k}\sum_{i_k} sv_kN_i = \sum_{i_k} sN_i,$$
$$E_k = \frac{1}{v_k}\sum_{i_k} sv_kS_{i_k} = \sum_{i_k} sS_{i_k}. \tag{2.5}$$

These terms were added to the ship population densities once per simulation day according to $S_k + I_k - E_k$.

The parameters a and all mortality rates (i.e. in-ship mortality μ_k, in-port mortality μ_i in the scenario of no environmental variation and otherwise μ_{Temp}, μ_{Tm}, μ_{Sal}, μ_{Nit}, μ_{Phos} and μ_{Sil} for different environmental factors, electronic supplementary material, table S2) were estimated by model fitting (see below). The following parameters were assumed to be constant: in-port growth rate $r = 0.1\ \text{d}^{-1}$; in-port carrying capacity of the population $k = 1$ individual m^{-3}; port volume $v_i = 10^6\ \text{m}^3$; fraction of released/uploaded ballast water of total ballast tank capacity $s = 0.05$. The relationship between ballast tank capacity and port volume v_i/v_k ranged from 4×10^{-5} to 0.15 with a median of 8×10^{-3}. The values of the constant parameters were chosen based on educated guesses rather than on *in situ* measurements owing to the lack of data. Note that the choice of these values, although affecting the predicted absolute propagule pressure, did not influence the overall results qualitatively. For instance, a certain port would always be invaded before another one irrespective of the choice of these parameters. As a consequence, the absolute population densities and propagule pressures predicted in this study should be interpreted carefully.

(e) Simulations and model selection

Temporal developments of population densities N_i and S_k were calculated using the Euler method, which is a simple but efficient way of approximating ODEs. Each model version was parametrized using four simulation runs, starting at one of the four source regions in the native range (figure 1). A simulation run was initialized by setting the population density of the ports in a source region to the carrying capacity. In all other ports, initial population densities were zero. A source region was defined by the ports located in the direct vicinity of the sampling site in Ghabooli *et al.* [20,21] and represented by three to six ports (figure 1). Parametrization of the model was done by constructing two matrices of similarity proxies of native (rows) and non-native (columns) populations, one with F_{st} values obtained from Ghabooli *et al.* [20,21] and another one with invasion times. For the latter, we extracted the invasion time, which was the time when a non-native population exceeded a_{real}. If population density did not exceed a_{real}, invasion time was set to a maximum value.

Parametrization was done by applying the optimization algorithm 'simulated annealing' [33], which attempted to find the best fit between simulation results and F_{st} data calculated as the correlation coefficient between simulation results and F_{st} data. We thereby assumed that an early invasion time indicated frequent introductions of individuals, which should result in lower F_{st} values. In extreme cases, F_{st} should saturate at very high numbers of exchanged individuals, but this was unlikely to be the case here. Only a positive sign of the correlation coefficient was accepted as an improvement in model fit. Parametrization was repeated several times with varying initial settings and various numbers of iterations to avoid being trapped in a local minimum of the model fit landscape. The obtained parameter settings were used as starting points for further optimization runs to get confidence in calibration results. Model versions were compared among each other using Akaike's information criterion corrected for small sample sizes (AICc) [34] obtained from the regression between F_{st} values (electronic supplementary material, table S1) and invasion times. The number of parameters used for the AIC calculation was taken from the model rather than from the regression to include a penalty for more complex models. The model version and parametrization with the lowest AICc was selected as the best-fitting model. For each model fit, we calculated AIC weights (AICw) [34]. AICw can be interpreted as the weight of evidence in favour of a single model run being the best fit. We used AICw to investigate the importance of a single parameter by summing up the AICw of all model fits including a certain parameter. An AICw of one indicated a high relevance of that parameter setting.

In addition to the single best-fitting model, we determined the set of best-fitting models, which were those models with $\Delta\text{AICc} < 5$ compared to the best-fitting model. The set of best-fitting models were used to analyse the influence of parametrization on model results. This required an equivocal distribution of parameter values, which was not achieved by applying simulated annealing. We therefore tested all combinations of all parameters within a predefined range of the full parameter space. The resolution of the parameter ranges has to be comparatively coarse owing to the large number of possible permutations. For example, a variation of the eight parameters with only five different possible values resulted in more than 1.5 million model runs. Consequently, we restricted this procedure to the selection of the six μ_e values and tested 16 055 different parameter combinations.

The results of the best-fitting models were used to analyse the interaction of propagule pressure, which was the realized critical density, and the probability of invasion. The probability of invasion at a port was expressed as the proportion of successful invasions at that port among all best-fitting models (ΔAICc less than 5). The propagule pressure was calculated as the mean number of released individuals in a port for 10 days. The choice of a time period, although arbitrary, minimized influences of the highly variable shipping intensity on the calculation of propagule pressure. A change of the time period would result in a change of the mean propagule pressure. A commonly applied risk–release functional relationship [5,35] was fitted to compare the propagule pressure required for a successful invasion across different sites: $P(Inv) = x[1 - \exp(-yp^2)]$ with $P(Inv)$ being the invasion probability related to propagule pressure p under the constraint of an Allee effect, and x and y being fitted scale and shape parameters, respectively.

3. Results

The total number of ships leaving one of the United States (US) source regions during the study period 2007–2008 varied from 263 ships departing from Narragansett Bay to nearly 10 times that number leaving Chesapeake Bay ($n = 2437$). This was also reflected in the origin of ships entering European ports: in all cases, most ships came from Chesapeake Bay, and, in all but one case, more than 50% of the ship calls were from ports in Chesapeake Bay (electronic supplementary material, figure S4).

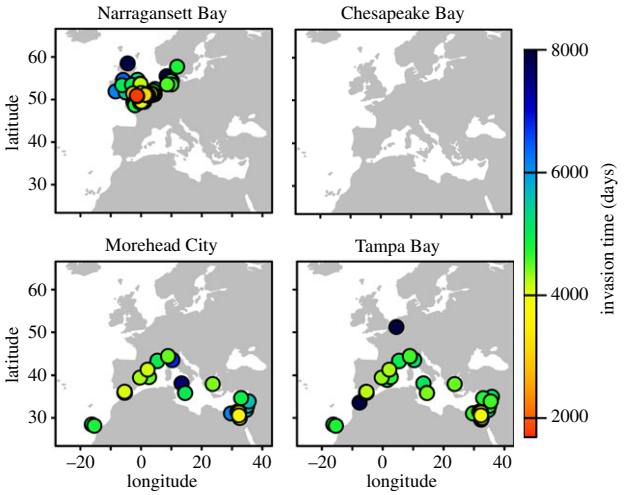

Figure 2. Predicted invasion times of *M. leidyi* in Europe obtained by the best-fitting model. Each panel shows simulation results starting from one of the four source regions. No invasion was observed starting from Chesapeake Bay.

The best-fitting scenario was obtained using a model with four environmental factors (annual mean temperature, salinity, phosphate and silicate) and considering four distinct ecotypes of *M. leidyi* as the initial condition ($R^2 = 0.65$, electronic supplementary material, table S2). Using this model version, invasions were successful in the northern European seas and in the Mediterranean Sea but not in the Black Sea (figure 2). Ignoring environmental conditions revealed a considerably worse model fit, whereas the consideration of only a single ecotype performed slightly worse (electronic supplementary material, table S2). In the following, we only analysed the results of the best-fitting model in more detail. The analysis of the set of best-fitting models revealed that the determination of the parameter values was often unambiguous in the sense that in most cases, a narrow range of the parameter values were superior, which indicated low uncertainty (electronic supplementary material, figure S5). Exceptions were a and μ_T, which showed a slightly broader range of values with similar fits.

Using the parametrization of the single best-fitting model, we calculated the critical density a_{real}, which gave us a map of suitability for each ecotype (electronic supplementary material, figure S6). The ports with the lowest a_{real} values were often those ports which were invaded along a clear latitudinal gradient (figure 2): populations originating from the northern US east coast established in northern European seas, whereas populations from the southern US east coast tended to establish at warmer ports in the Mediterranean Sea. However, we also found counterintuitive results: individuals from Tampa Bay established in the comparatively cold port of Antwerp, Belgium, probably owing to intense shipping, whereas individuals from Chesapeake Bay did not establish in any European port despite high shipping intensity. The analysis of the evolution of propagule pressure revealed that the number of individuals released into

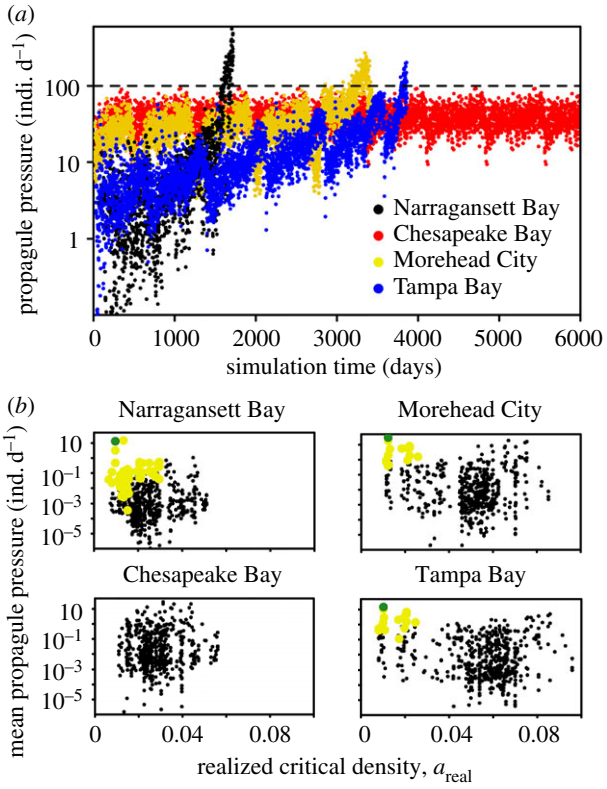

Figure 3. Interaction of propagule pressure and realized critical density of the best-fitting model at European ports before the very first invasion happened. (*a*) The temporal development of the propagule pressure indicated by the number of released individuals per day in European ports is shown for the four invasion scenarios. The oscillations reflect the 2-year period of shipping data availability. (*b*) Scatter plots of mean propagule pressure released at a port and the realized critical density of the same port. Propagule pressure was averaged over a 10-day period before the very first establishment of *M. leidyi* in any European port. The port of the first invasion (green) and the subsequently invaded ports are highlighted (yellow).

European ports originating from Chesapeake Bay was initially two to three orders of magnitude higher compared to those from other source populations (figure 3*a*). However, propagule pressure from Chesapeake Bay did not change substantially over the course of the whole simulation and always remained below the level of 100 individuals per day. By contrast, propagule pressure from Narragansett Bay, Morehead City or Tampa Bay started at lower levels but thereafter rose continuously with ongoing simulations until they exceeded this threshold.

Interestingly, the propagule pressure released into European ports increased with time (figure 3*a*), despite recurrent shipping intensities and stable environmental conditions. This occurred because simulations started with a low number of native populations (three to six ports), which quickly spread to neighbouring ports of similar suitability. The propagule pressure at a single European port was then the result of the coincident arrival of individuals released by various ships from a growing number of source ports. For instance, individuals from Tampa Bay first established three new populations within the USA before arriving in the Mediterranean Sea, and those from Morehead City established five new populations, three in the USA, one in Panama and one Hong Kong, before arriving in European waters. This was not the case for individuals native to Chesapeake Bay, which did not establish new populations outside this region.

On average, propagule pressure imposed on European ports was equally high irrespective of the source region, whereas the mean realized critical density was comparatively high for individuals from Morehead City and Tampa Bay (figure 3*b*). However, in all scenarios except Chesapeake Bay, at least one port existed with both low realized critical density and high propagule pressure, which was the port invaded first (see green dots in figure 3*b*). High propagule pressure from Chesapeake Bay was mostly imposed on ports with a high realized critical density, which hindered the establishment of new populations. Once an initial founding population was established, *M. leidyi* invaded other nearby ports even if they had a realized critical density comparable to those in the Chesapeake Bay scenario, but in contrast, the establishment was supported by individuals from the nearby founding population, which enabled the species to invade less suitable habitats as well.

The systematic analysis of the full parameter space revealed that many parameter settings provided similar fits. To test the robustness of our findings, we therefore compared the results of all top fitting models ($n = 197$), which are those with an AICc deviating by less than five from the overall best-fitting model. This set of best-fitting models illustrated that the Baltic Sea was invaded from Narragansett Bay in 94% of all cases (electronic supplementary material, table S3). Similarly, individuals from Tampa Bay and Morehead City always invaded the Mediterranean Sea, whereas individuals from Chesapeake Bay were only rarely successful in Europe (only 2% of all cases). Model selection had very little effect on these findings, as frequencies did not change. For example, using the best 500 model simulations (instead of 197) resulted in a success rate of 82% from Narragansett Bay to the Baltic Sea, 100% from Tampa Bay or Morehead City to the Mediterranean Sea, and only 6% from Chesapeake Bay. The invasion patterns (electronic supplementary material, table S3) were very consistent with data of genetic similarity from Ghabooli *et al.* [20,21] (Pearson's correlation coefficient 0.84 between data shown in the electronic supplementary material, tables S1 and S3).

The risk–release relationships demonstrated that invasion probability increased rapidly with propagule pressure below *ca* 30 individuals d^{-1}, and levelled off thereafter (figure 4). Averaged over source regions, an invasion probability of 50% was achieved with 27 individuals released d^{-1}. However, it was also clear that the risk–release relationship was highly variable, depending on environmental heterogeneity. That is, high propagule pressure alone did not necessarily result in a high invasion probability. The risk–release relationship was steeper when we only considered sites of best environmental conditions, i.e. the 50% invasion probability could be obtained with the release by 17 individuals d^{-1} when only sites with an a_{real} less than 0.01 were considered (figure 4).

4. Discussion

The spread of non-native species by means of global transportation is expected to surge globally [36] but can be complex owing to the large number of individual vehicles and the multitude of routes they can take. Although we applied our model to the population and spreading dynamics

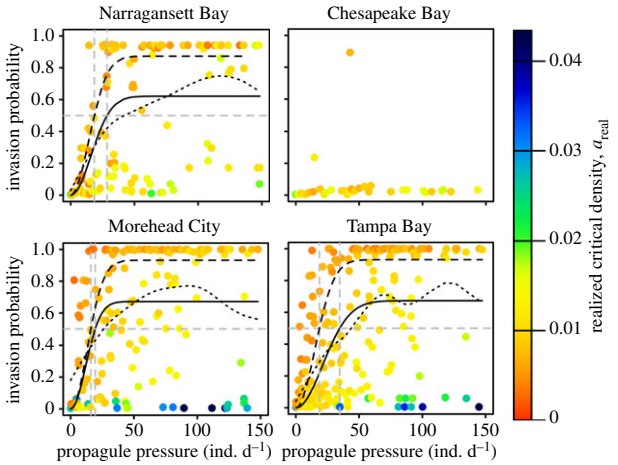

Figure 4. Risk–release relationships (black lines) of invasion probability and mean propagule pressure of the set of best-fitting models. The risk–release relationship was fitted to all data (solid line) or only to ports providing good environmental conditions (dashed line, $a_{real} < 0.01$). An invasion probability of 50% (grey lines) is, on average, achieved with a propagule pressure of 27 (17 considering only ports with good environmental conditions) individuals d^{-1}. Using a smoothed spline (dotted line) gives a similar relationship. (Online version in colour.)

of *M. leidyi*, our study provides a number of important insights into the spread of non-native species in complex networks in general. We show that invasion success depends critically upon the interactions of global transport and local population dynamics. Owing to the high intensity of ship traffic, individuals were frequently introduced into numerous ports simultaneously, though often at densities, which were insufficient to found a new population. Invasion success depends critically on the coincident arrival of individuals from various source populations, which may be native or non-native, at ports providing suitable conditions. As global ship traffic continues to increase, with ever more complicated shipping networks, there will exist additional opportunities for invasions [36].

We show that the spread of *M. leidyi* was driven by complex source–sink dynamics [37]: populations in ballast water tanks and in most ports represent sink populations as they faced negative growth and could only exist because of regular input of individuals from viable source populations. However, if many sink populations merge—as may happen when many ships release individuals at similar times in the same port—the merged population in the port may overcome the realized critical density and establish a non-native population. The ships releasing these individuals do not have to originate directly from the same source population. Indeed, ships often stop at intermediate sites and may take different routes to the same destination [27]. It is therefore difficult to precisely predict new establishments based only on direct port-to-port comparisons [12]. Thus, spreading dynamics of species transported in such a complex network can be much more complicated than the often-assumed, single invasion event [8].

The complexity of numerous individual ship movements and ballast water releases, and population dynamics (which depend on multiple factors) impedes a thorough analysis of spreading dynamics. We therefore developed a model to capture the main processes under investigation, which ignored aspects potentially important for more specific case studies such as directed ballast water transport or life-history dynamics. We intentionally kept the model simple to ease our understanding of resulting simulations, which comes at the cost of simplifying shipping and population dynamics. Although this might affect the interpretation of the simulated spread of *M. leidyi* or individual port invasion probabilities, it did not influence our overall conclusions about the interaction of global transportation and local population dynamics.

The probability of invasion clearly increased with propagule pressure. On average, there was a 50% probability of invasion when a critical propagule pressure of 27 individuals d^{-1} was released (figure 4). However, the exact value of the critical propagule pressure needs to be interpreted carefully for three reasons. First, the concept of propagule pressure is poorly defined when individuals of the same species were released at quasi-continuous rates, such as with planktonic species. Second, we assumed a homogeneous distribution of individuals throughout the entire port immediately after the release of individuals. Third, abundances cannot be accurately predicted in our approach owing to an absence of abundance data, which could be used to assess the reliability and robustness of parameter selection. Hence, absolute numbers calculated here are difficult to compare with measured densities. The risk–release relationship is of considerable practical interest [9,38], but our study highlights the difficulty of estimating it owing to interactions with local environmental conditions. A high propagule pressure does not necessarily lead to a successful invasion if the releasing site is of poor environmental quality, which is indicated by a high a_{real} in figure 4; considering only suitable sites results in a steeper increase (dashed line in figure 4) as compared to a curve fitted to all sites (solid line in figure 4). This difference introduces spatial variation in the shape of the risk–release relationship, which has to be taken into account when interpreting the curve.

Despite the recognized importance of propagule pressure [6,38] for the prediction of an invasion event, high propagule pressure by itself does not guarantee successful invasion. For instance, by far the highest shipping intensity in our study originated from Chesapeake Bay and resulted in high propagule pressure imposed on European ports, a magnitude higher in fact than that associated with Narragansett Bay (figure 3*a*). But this did not result in a successful invasion. The reason was twofold: high numbers of individuals were only released into ports with less suitable conditions (i.e. high realized critical density) (figure 3*b*, electronic supplementary material, figure S6) and individuals from the native source population were not able to establish in other ports, which may have served as 'bridgehead' populations to support the spreading process [39]. Starting from other source regions allowed the species to establish outside Europe, resulting in the progressive increase in propagule pressure released into European ports (figure 3*a*). In addition, more individuals were released into the most suitable European ports (green dots in figure 3*b*), which allowed populations to establish despite less favourable environmental conditions.

Our results support conclusions drawn by Ghabooli *et al.* [21] and Reusch *et al.* [22] of multiple introductions into European waters, as all of our best-fitting models revealed dominant northern and southern invasion pathways. But

the model failed to simulate the spread of *M. leidyi* into the Black Sea, where the species was first observed in Europe [15]. In the Black Sea, a_{real} was lowest for individuals arriving from Chesapeake Bay or Narragansett Bay (electronic supplementary material, figure S6), but our simulations failed to account for individuals from these regions establishing in the Mediterranean Sea or the Black Sea (figure 2). The discrepancy between model predictions and field data highlights a drawback inherent to all studies trying to reconstruct spread dynamics: usually, the likelihoods of different spreading scenarios are analysed, although a high probability does not have to indicate true patterns. It is also worth mentioning the recent hypothesis [7] that mortality during transport may not be stochastic, but selective, retaining additive genetic variance in the surviving population that would help avoid negative consequences of low propagule pressure. While chances are low, alternative spread scenarios may, in fact, represent the true invasion pathway. However, definitive evidence of the true invasion pathways was missing. In addition, we lacked information pertaining to shipping intensity of inland canals in Europe, nor did we consider other means of transportation such as water currents [18]. We can, however, not rule out the possibility that the actual spread of *M. leidyi* was driven by developments of propagule pressure more complex than considered here, because of high variation in releases and potential unidirectional transport of ballast water [40].

In conclusion, this study illustrated how the interactions of spatio-temporal variation in propagule pressure and local population dynamics may affect the spread of a non-native species in a complex, global shipping network. The propagule pressure imposed at one site can be the result of complex spreading dynamics along different routes. The number of individuals transported along a single route at one time may be very low and insufficient for the establishment of a new population, but the combined release of several of these sink populations at the same port may result in a sufficiently high density to overcome the Allee threshold. This may not only hold true for species transported in ballast water, but similar dynamics can be expected for other transportation networks such as commodity flows and other taxonomic groups (such as insects or plants), which are frequently transported in larger quantities. Expanding global shipping traffic highlights that the complex network analysed here may become the norm rather than the exception for facilitating global spread of non-native species.

Data accessibility. Data (C code of the model and the parametrization method together with the required input files) is available from the Dryad Digital Repository: https://doi.org/10.5061/dryad.2c5k96n [41].

Authors' contributions. H.S. and B.B. designed the study and developed the model. H.S. did all coding, performed all modelling and statistical analyses. S.G., H.J.M. and T.S. provided results of genetic analysis. All authors contributed to the discussion of results, refinement of analyses and helped drafting the manuscript.

Competing interests. We declare we have no competing interests.

Funding. H.S. and B.B. acknowledge support from the Volkswagen Foundation. H.S. was additionally supported by the German Research Foundation (DFG, grant no. SE 1891/2-1). E.B. acknowledges funding from the Alexander von Humboldt Sofja Kovalevskaja Award and H.J.M. from an NSERC Discovery grant and Canada Research Chair. Research of T.S. was performed within the framework of the Ministry of Education and Science of the Russian Federation (Minobrnauka)—0149-2019-0010.

References

1. CBD. 2014 *Global biodiversity outlook 4*. Montréal, Canada: Secretariat of the Convention on Biological Diversity.
2. Hulme PE. 2009 Trade, transport and trouble: managing invasive species pathways in an era of globalization. *J. Appl. Ecol.* **46**, 10–18. (doi:10.1111/j.1365-2664.2008.01600.x)
3. Turbelin AJ, Malamud BD, Francis RA. 2017 Mapping the global state of invasive alien species: patterns of invasion and policy responses. *Glob. Ecol. Biogeogr.* **26**, 78–92. (doi:10.1111/geb.12517)
4. Chapman DS, Makra L, Albertini R, Bonini M, Páldy A, Rodinkova V, Šikoparija B, Weryszko-Chmielewska E, Bullock JM. 2016 Modelling the introduction and spread of non-native species: international trade and climate change drive ragweed invasion. *Glob. Chang. Biol.* **22**, 3067–3079. (doi:10.1111/gcb.13220)
5. Leung B, Drake JM, Lodge DM. 2004 Predicting invasions: propagule pressure and the gravity of Allee effects. *Ecology* **85**, 1651–1660.
6. Simberloff D. 2009 The role of propagule pressure in biological invasions. *Annu. Rev. Ecol. Evol. Syst.* **40**, 81–102. (doi:10.1146/annurev.ecolsys.110308.120304)
7. Briski E, Chan FT, Darling JA, Lauringson V, MacIsaac HJ, Zhan A, Bailey SA. 2018 Beyond propagule pressure: importance of selection during the transport stage of biological invasions. *Front. Ecol. Environ.* **16**, 345–353. (doi:10.1002/fee.1820)
8. Cassey P, Delean S, Lockwood JL, Sadowski J, Blackburn TM. 2018 Dissecting the null model for biological invasions: a meta-analysis of the propagule pressure effect. *PLoS Biol.* **16**, e2005987. (doi:10.1371/journal.pbio.2005987)
9. Carlton JT *et al*. 2011 Assessing the relationship between propagule pressure and invasion risk in ballast water. Report of the National Research Council of the National Academies. Washington, DC: The National Academic Press.
10. Tobin PC, Whitmire SL, Johnson DM, Bjornstad ON, Liebhold AM. 2007 Invasion speed is affected by geographical variation in the strength of Allee effects. *Ecol. Lett.* **10**, 36–43.
11. Paini DR, Yemshanov D. 2012 Modelling the arrival of invasive organisms via the international marine shipping network: a Khapra beetle study. *PLoS ONE* **7**, e44589. (doi:10.1371/journal.pone.0044589)
12. Keller RP, Drake JM, Drew MB, Lodge DM. 2011 Linking environmental conditions and ship movements to estimate invasive species transport across the global shipping network. *Divers. Distrib.* **17**, 93–102. (doi:10.1111/j.1472-4642.2010.00696.x)
13. Seebens H, Schwartz N, Schupp PJ, Blasius B. 2016 Predicting the spread of marine species introduced by global shipping. *Proc. Natl Acad. Sci. USA* **113**, 5646–5651. (doi:10.1073/pnas.1524427113)
14. Shiganova TA. 1998 Invasion of the Black Sea by the ctenophore *Mnemiopsis leidyi* and recent changes in pelagic community structure. *Fish. Oceanogr.* **7**, 305–310. (doi:10.1046/j.1365-2419.1998.00080.x)
15. Shiganova TA, Mirzoyan Z, Studenikina E, Volovik SP, Siokou-Frangou I, Zervoudaki I, Christou E, Skirta A, Dumont H. 2001 Population development of the invader ctenophore *Mnemiopsis leidyi*, in the Black Sea and in other seas of the Mediterranean basin. *Mar. Biol.* **139**, 431–445. (doi:10.1007/s002270100554)
16. Faasse MA, Bayha KM. 2006 The ctenophore *Mnemiopsis leidyi* A. Agassiz 1865 in coastal waters of the Netherlands?: an unrecognized invasion? *Aquat. Invasions* **1**, 270–277.
17. Javidpour J, Sommer U, Shiganova TA. 2006 First record of *Mnemiopsis leidyi* A. Agassiz 1865 in the Baltic Sea. *Aquat. Invasions* **1**, 299–302. (doi:10.3391/ai.2006.1.4.17)
18. Jaspers C *et al*. 2018 Ocean current connectivity propelling the secondary spread of a marine invasive comb jelly across western Eurasia. *Glob.*

Ecol. Biogeogr. **27**, 814–827. (doi:10.1111/geb.12742)

19. Fuentes V, Atienza D, Gili J-M, Purcell J. 2009 First records of *Mnemiopsis leidyi* A. Agassiz 1865 off the NW Mediterranean coast of Spain. *Aquat. Invasions* **4**, 671–674. (doi:10.3391/ai.2009.4.4.12)
20. Ghabooli S, Shiganova TA, Briski E, Piraino S, Fuentes V, Thibault-Botha D, Angel DL, Cristescu ME, Macisaac HJ. 2013 Invasion pathway of the Ctenophore *Mnemiopsis leidyi* in the Mediterranean Sea. *PLoS ONE* **8**, e81067. (doi:10.1371/journal.pone.0081067)
21. Ghabooli S, Shiganova TA, Zhan A, Cristescu ME, Eghtesadi-Araghi P, MacIsaac HJ. 2011 Multiple introductions and invasion pathways for the invasive ctenophore *Mnemiopsis leidyi* in Eurasia. *Biol. Invasions* **13**, 679–690. (doi:10.1007/s10530-010-9859-8)
22. Reusch TBH, Bolte S, Sparwel M, Moss AG, Javidpour J. 2010 Microsatellites reveal origin and genetic diversity of Eurasian invasions by one of the world's most notorious marine invader, *Mnemiopsis leidyi* (Ctenophora). *Mol. Ecol.* **19**, 2690–2699. (doi:10.1111/j.1365-294X.2010.04701.x)
23. Bolte S *et al.* 2013 Population genetics of the invasive ctenophore *Mnemiopsis leidyi* in Europe reveal source-sink dynamics and secondary dispersal to the Mediterranean Sea. *Mar. Ecol. Prog. Ser.* **485**, 25–36. (doi:10.3354/meps10321)
24. Lehtiniemi M, Lehmann A, Javidpour J, Myrberg K. 2012 Spreading and physico-biological reproduction limitations of the invasive American comb jelly *Mnemiopsis leidyi* in the Baltic Sea. *Biol. Invasions* **14**, 341–354. (doi:10.1007/s10530-011-0066-z)
25. Tyrrell T. 1999 The relative influences of nitrogen and phosphorus on oceanic primary production. *Nature* **400**, 525–531.
26. Seebens H, Gastner MT, Blasius B. 2013 The risk of marine bioinvasion caused by global shipping. *Ecol. Lett.* **16**, 782–790. (doi:10.1111/ele.12111)
27. Kaluza P, Kölzsch A, Gastner MT, Blasius B. 2010 The complex network of global cargo ship movements. *J. R. Soc. Interface* **7**, 1093–1103. (doi:10.1098/rsif.2009.0495)
28. ABS. 2011 *Ballast water treatment advisory*. Houston, TX: ABS (American Bureau of Shipping).
29. Lewis MA, Kareiva P. 1993 Allee dynamics and the spread of invading organisms. *Theor. Popul. Biol.* **43**, 141–158.
30. Taylor CM, Hastings A. 2005 Allee effects in biological invasions. *Ecol. Lett.* **8**, 895–908. (doi:10.1111/j.1461-0248.2005.00787.x)
31. Wonham MJ, Lewis MA, MacIsaac HJ. 2005 Minimizing invasion risk by reducing propagule pressure: a model for ballast-water exchange. *Front. Ecol. Environ.* **3**, 473–478.
32. Gollasch S, Lenz J, Dammer M, Andres HG. 2000 Survival of tropical ballast water organisms during a cruise from the Indian Ocean to the North Sea. *J. Plankton Res.* **22**, 923–937.
33. Kirkpatrick S, Gelatt CD, Vecchi MP. 1983 Optimization by simulated annealing. *Science* **220**, 671–680. (doi:10.1126/science.220.4598.671)
34. Burnham KP, Anderson DR. 2004 Model selection and inference – a practical information-theoretic approach. *Sociol. Methods Res.* **33**, 261–304.
35. Gertzen EL, Leung B, Yan ND. 2011 Propagule pressure, Allee effects and the probability of establishment of an invasive species (*Bythotrephes longimanus*). *Ecosphere* **2**, 1–17. (doi:10.1890/ES10-00170.1)
36. Sardain A, Sardain E, Leung B. 2019 Global forecasts of shipping traffic and biological invasions to 2050. *Nat. Sustain.* **2**, 274–282. (doi:10.1038/s41893-019-0245-y)
37. Amarasekare P, Nisbet RM. 2001 Spatial heterogeneity, source-sink dynamics, and the local coexistence of competing species. *Am. Nat.* **158**, 572–584.
38. Lockwood JL, Cassey P, Blackburn T. 2005 The role of propagule pressure in explaining species invasions. *Trends Ecol. Evol.* **20**, 223–228. (doi:10.1016/j.tree.2005.02.004)
39. Bertelsmeier C, Liebhold AM, Brockerhoff EG, Ward D, Keller L, States U, Zealand N. 2018 Recurrent bridgehead effects accelerate global alien ant spread. *Proc. Natl Acad. Sci. USA* **115**, 5486–5491. (doi:10.1073/pnas.1801990115)
40. Verling E, Ruiz GM, Smith LD, Galil B, Miller AW, Murphy KR. 2005 Supply-side invasion ecology: characterizing propagule pressure in coastal ecosystems. *Proc. R. Soc. B* **272**, 1249–1256. (doi:10.1098/rspb.2005.3090)
41. Seebens H, Briski E, Ghabooli S, Shiganova T, MacIsaac HJ, Blasius B. 2019 Data from: Non-native species spread in a complex network: the interaction of global transport and local population dynamics determines invasion success. Dryad Digital Repository. (https://doi.org/10.5061/dryad.2c5k96n)